

Transport and metabolism of MitoQ₁₀, a mitochondria-targeted antioxidant, in Caco-2 cell monolayers

Yan Li, J. Paul Fawcett, Hu Zhang and Ian G. Tucker

Abstract

Mitoquinone (MitoQ₁₀ mesylate) is a mitochondria-targeted antioxidant formulated for oral administration in the treatment of neurodegenerative diseases. We have investigated the absorption and metabolism of MitoQ₁₀ in Caco-2 cell monolayers. The intracellular accumulation of MitoQ₁₀ was 18–41% of the total amount of MitoQ₁₀ added. Some of the intracellular MitoQ₁₀ was reduced to mitoquinol and subsequently metabolized to glucuronide and sulfate conjugates. Transport of MitoQ₁₀ was polarized with the apparent permeability (P_{app}) from basolateral (BL) to apical (AP) ($P_{appBL \rightarrow AP}$) being >2.5-fold the P_{app} from apical to basolateral ($P_{appAP \rightarrow BL}$). In the presence of 4% bovine serum albumin on the basolateral side, the $P_{appAP \rightarrow BL}$ value increased 7-fold compared with control. The $P_{appBL \rightarrow AP}$ value decreased by 26, 31 and 61% in the presence of verapamil 100 μ M, ciclosporin 10 and 30 μ M, respectively, whereas the $P_{appAP \rightarrow BL}$ value increased 71% in the presence of ciclosporin 30 μ M. Apical efflux of mitoquinol sulfate and mitoquinol glucuronide conjugates was significantly decreased by ciclosporin 30 μ M and the breast cancer receptor protein (BCRP) inhibitor, reserpine 25 μ M, respectively. These results suggested that the bioavailability of MitoQ₁₀ may be limited by intracellular metabolism and the action of P-glycoprotein and BCRP. However, the dramatic increase in absorptive P_{app} in the presence of bovine serum albumin on the receiver side suggests these barrier functions may be less significant in-vivo.

Introduction

Mitochondrial oxidative damage is implicated in various diseases including Parkinson's disease, Friedreich's ataxia, diabetes and certain types of cancer (Murphy & Smith 2000). Targeted delivery of bioactive molecules to mitochondria may be a new therapeutic strategy for these conditions (Murphy & Smith 2000; Smith et al 2003). Mitoquinone (10-(4,5-dimethoxy-2-methyl-3,6-dioxo-1,4-cyclohexadien-1-yl)decyl) triphenylphosphonium mesylate (MitoQ₁₀ mesylate) is currently undergoing development as a mitochondria-targeted antioxidant where the active form is mitoquinol produced by intracellular reduction (James et al 2005) (Figure 1). The cationic nature of MitoQ₁₀ promotes its selective accumulation within mitochondria due to the large mitochondrial membrane potential (negative inside) (Kelso et al 2001; Smith et al 2003). This imparts a several hundredfold increase in potency at preventing mitochondrial oxidative damage compared with an untargeted antioxidant such as idebenone (Kelso et al 2001; Jauslin et al 2003; Asin-Cayuella et al 2004; Adlam et al 2005). Currently, mitoquinone is undergoing Phase II clinical trials in New Zealand for treatment of Parkinson's disease.

Recently, it has been recognized that several neuroprotective agents require a slower and more prolonged administration schedule to produce optimal neuroprotective effects (Stoof et al 1999; Nyholm 2006). Oral regimens are generally appropriate for this purpose. In addition, oral regimens are more acceptable due to their greater safety, cost effectiveness, convenience and ability to improve life quality (DeMario & Ratain 1998; Bleyer & Danielson 1999). Although animal studies suggest oral delivery of MitoQ₁₀ is feasible (Smith et al 2003; Adlam et al 2005), a better understanding of intestinal absorption mechanisms of this permanently cationic compound is required. Such mechanism studies can be addressed through in-vitro studies of drug absorption.

School of Pharmacy, University
of Otago, Dunedin, P.O. Box 913,
New Zealand

Yan Li, J. Paul Fawcett,
Hu Zhang, Ian G. Tucker

Correspondence: Y. Li, School
of Pharmacy, University of
Otago, Dunedin, P.O. Box 913,
New Zealand. E-mail:
yan.li@stonebow.otago.ac.nz

Acknowledgements: The
authors would like to thank
Mr Len Stevenson for his
technical support in LC-MS
maintenance.

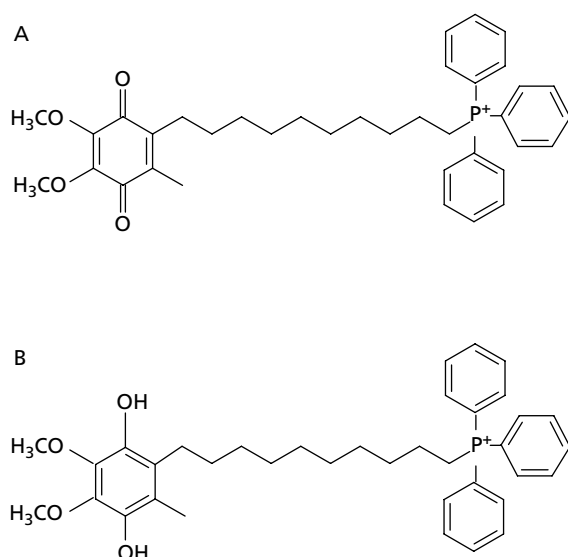


Figure 1 Chemical structures of MitoQ₁₀ (A) and mitoquinol (B).

The human intestinal Caco-2 cell monolayer is a proven model of drug absorption in the development of potential drug candidates (Artursson & Karlsson 1991; Yee 1997; Matsson et al 2005). Functional expression of various drug transporters and metabolic enzymes in Caco-2 cells allows elucidation of drug absorption pathways and intestinal metabolic profiles (Gan & Thakker 1997; Artursson et al 2001). The information provided is useful in guiding formulation design and predicting potential drug–drug/food–drug interactions. We have investigated the transport and metabolism of MitoQ₁₀ across Caco-2 cell monolayers.

Materials and Methods

Materials

Mitoquinone and [³H]mitoquinone mesylate (sp. act. 11.7 mCi mmol⁻¹; radiochemical purity, 98.5%) were provided by Professor Robin R. Smith of the Chemistry Department, University of Otago, New Zealand. Caco-2 cells were obtained from the American Type Culture Collection (Rockville, MD). Dulbecco's modified Eagle's medium (DMEM), Hank's Balanced Salt Solution (HBSS), fetal bovine serum (FBS), trypsin-EDTA, non-essential amino acids, and penicillin-streptomycin-glutamine were all from Life Technologies (Auckland, New Zealand). Bovine serum albumin (BSA), N-[2-hydroxyethyl]piperazine-N'-[4-butanefulfonic acid] (HEPES), β-glucuronidase (from *Helix pomatia*), sulfatase (from *H. pomatia*), ciclosporin (cyclosporine), verapamil, indometacin, reserpine and decynium 22 were purchased from Sigma Chemical Co. (Sydney, Australia). [¹⁴C]Mannitol (sp. act. 51 mCi mmol⁻¹; radiochemical purity, 98.6%) was purchased from Amersham Pharmacia (Auckland, New Zealand). Transwell inserts and plates (12 mm i.d., 0.4-μm pore size, 1.13 cm², polycarbonate filters) were obtained from Corning Costar Corp (Cambridge, MA). Acetonitrile (HPLC

grade) was purchased from Lab Supply Co. (Auckland, New Zealand). Distilled water, prepared from demineralized water, was used throughout the study. Other reagents were of analytical grade.

Preparation of mitoquinol mesylate

Mitoquinol mesylate was prepared according to James et al (2005). To a solution of mitoquinone mesylate (1 mM) in methanol (1.0 mL) was added a few mg NaBH₄. After incubation on ice in the dark for 5 min, excess NaBH₄ was consumed with 10% (v/v) methanesulfonic acid (0.2 mL). The complete conversion of MitoQ₁₀ to mitoquinol was confirmed by LC-MS analysis.

Cell culture

Caco-2 cells at passage 26 were cultured in complete DMEM containing 10% FBS, 1% penicillin-streptomycin-glutamine and 1% nonessential amino acids under an atmosphere of 5% CO₂/95% air at 37°C and 95% relative humidity. Caco-2 cells at 80–90% confluence were split with 0.05% trypsin-EDTA and seeded into Transwell inserts at a density of 2 × 10⁵ cells/insert. The medium was replaced every two days until 21–26 days. Transepithelial electrical resistance (TEER) (Ω•cm²) of the monolayers was measured at room temperature using a Millicell-ERS apparatus (Millipore Corp. Bedford, MA).

Bidirectional transport studies

Monolayers were washed twice with HBSS at 37°C before experiments. For apical (AP) to basolateral (BL) transport, 0.5 mL transport buffer (HBSS with 25 mM HEPES and 25 mM glucose at pH 7.4) containing MitoQ₁₀ (2.5–30 μM) was added to the apical side, and 1.5 mL transport buffer to the basolateral side. For basolateral to apical transport, 1.5 mL MitoQ₁₀ solution (2.5–30 μM) was added to the basolateral side and 0.5 mL transport buffer to the apical side. The effect of various compounds on MitoQ₁₀ transport was investigated by adding them to the mitoquinone solution (10 μM). To investigate the effect of plasma protein binding on apical to basolateral transport, transport buffer containing 4% (w/v) BSA was added to the basolateral side. After incubating for 0.5, 1, 1.5 and 2 h at 37°C, a sample (0.4 mL) was collected from the receiver side and replaced by 0.4 mL prewarmed transport buffer or 4% BSA in buffer. All samples were stored at –80°C until analysis. Monolayer integrity was confirmed by TEER value > 400 Ω•cm² and transepithelial transport of [¹⁴C]mannitol < 1%/h. A mass balance study was carried out separately using [³H]MitoQ₁₀ mesylate.

Cellular accumulation and metabolism studies

Following transport studies, monolayers were rinsed with 2 × 2 mL ice-cold HBSS. The washing buffer was subsequently monitored for MitoQ₁₀ by LC-MS. Caco-2 cells were scraped into a 1.5-mL centrifuge tube and 1.0 mL ice-cold acetonitrile added. Mixtures were vigorously vortexed for 10 min and then briefly sonicated in an ice bath. After

centrifugation at 12000 *g* for 15 min, supernatants were collected and 20 μ L injected into the LC-MS system for analysis. Cellular protein concentration in each culture dish was determined using the bicinchoninic acid method, and the cellular uptake of MitoQ₁₀ was expressed as ng (mg cellular protein)⁻¹. The average intracellular concentration of MitoQ₁₀ in Caco-2 cells was estimated using an average Caco-2 cell volume of 25 pL and an average cell density of 2.1×10^5 cm⁻² as reported by Doppenschmitt et al (1999).

The presence of phase II metabolites of MitoQ₁₀ was investigated by analysis after enzymatic hydrolysis. Samples (100 μ L) of cellular and receiver buffer contents at 2 h were incubated with and without β -glucuronidase (4000 U mL⁻¹) or sulfatase (4000 U mL⁻¹) in 0.2 mL 0.1 M acetate buffer (pH 5.0) at 37°C for 12 h. After cooling, ice-cold acetonitrile (0.4 mL) was added and the mixtures vigorously vortexed. After centrifugation at 12000 *g* for 15 min, supernatants were collected and analysed by LC-MS.

LC-MS analysis

Liquid chromatography was carried out on a reversed-phase C18 column (2.0 mm i.d. \times 150 mm, 5 μ m, Phenomenex) using 44% acetonitrile:56% water containing 0.1% formic acid (pH 2.8) as mobile phase at a flow rate of 0.2 mL min⁻¹. Detection was by an LCQ Deca ion trap mass spectrometer equipped with a TSP4000 HPLC pump and a TSP AS3000 autosampler (Finnigan, Austin, TX). Electrospray ionization in the positive ion mode was employed. Mass spectrometer parameters were: source spray voltage, 5 kV; capillary voltage, 46 V; heated capillary temperature, 150°C; sheath gas (nitrogen), 50 U. The MS² product ion spectra were produced by collision induced dissociation of the target molecular ions with optimized relative collision energy of 45% and isolation width (*m/z*) of 1. Xcalibur version 1.2 (Finnigan) was used for data manipulation. The assay was linear in the concentration range 5–500 ng mL⁻¹, with acceptable accuracy (85–115% of true values) and precision (intra- and inter-day coefficients of variation < 15%).

Data analysis

All data are expressed as mean \pm s.d. Transport of MitoQ₁₀ through Caco-2 cell monolayers was expressed as apparent permeability coefficient (P_{app} , cm s⁻¹), calculated using equation 1:

$$P_{app} = (\Delta Q / \Delta t) \times 1/A \times 1/C_0 \quad (1)$$

where ΔQ is the amount of MitoQ₁₀ appearing in the receiver chamber (μ mol), Δt the time of incubation (s), *A* the surface area of the membrane (1 cm²), and *C*₀ the initial loading concentration in the donor chamber (μ M). The efflux ratio of MitoQ₁₀ was determined as:

$$\text{Efflux ratio} = P_{appBL \rightarrow AP} (\text{Mean}) / P_{appAP \rightarrow BL} (\text{Mean}) \quad (2)$$

where $P_{appBL \rightarrow AP}$ and $P_{appAP \rightarrow BL}$ are the mean P_{app} values for transport in the basolateral to apical and apical to basolateral direction, respectively.

Differences in mean kinetic parameters were tested by one-way analysis of variance with a post-hoc test (Dunnett's multiple comparison test). Student's unpaired *t*-test was conducted for comparison between two groups and significance was set at a level of $P < 0.05$.

Results

Cellular accumulation of MitoQ₁₀

The apical and basolateral uptake of MitoQ₁₀ by Caco-2 cells was linear in the concentration range 2.5–30 μ M (Figure 2), with the basolateral uptake being 2–5-fold higher than the apical uptake at the same loading concentration. With apical loading of 5 μ M MitoQ₁₀, the uptake was found to be approximately 9.7×10^{-5} pmol pL⁻¹ after 2 h, whereas for basolateral loading it was 2.4×10^{-4} pmol pL⁻¹. The percentage apical uptake of MitoQ₁₀ was relatively constant at all concentrations, being 26 \pm 3, 25 \pm 3, 18 \pm 1, 27 \pm 3 and 25 \pm 3% of the total added amount at the loading concentrations of 2.5, 5, 10, 20 and 30 μ M, respectively. At these concentrations the percentage basolateral uptake was more variable being 41 \pm 5, 31 \pm 3, 18 \pm 2, 35 \pm 3 and 41 \pm 5% of the loading dose. At equilibrium, the intracellular (average)/extracellular MitoQ₁₀ concentration ratios were 90 \pm 12, 140 \pm 16, 43 \pm 6, 70 \pm 15 and 47 \pm 8 after 2-h apical loading of 2.5, 5, 10, 20 and 30 μ M, respectively.

Metabolism of MitoQ₁₀ by Caco-2 cells

Incubation of MitoQ₁₀ with Caco-2 cell monolayers produced two intracellular species with protonated molecular ions at *m/z* 585 (M1) and 665 (M2) (Figure 3a), and two species in extracellular buffer with molecular ions at *m/z* 761 (M3) and 665 (M2) (Figure 3b). M1, M2 and M3 were tentatively identified as mitoquinol (*m/z* 585), monosulfated mitoquinol (*m/z* 665) and monoglucuronidated mitoquinol (*m/z* 761). When extracellular buffer was treated with β -glucuronidase, the M3 peak

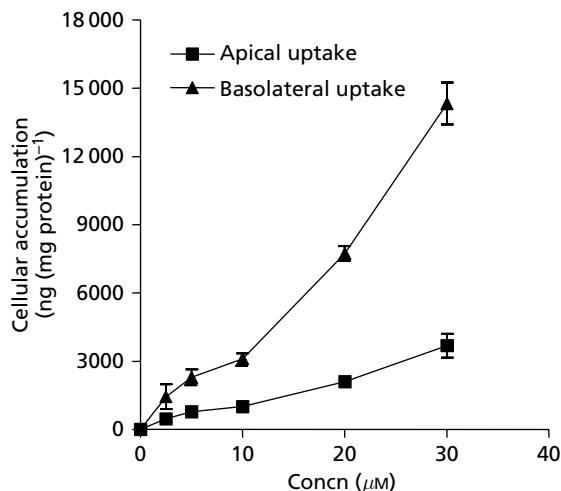


Figure 2 Cellular accumulation of MitoQ₁₀ 2 h after apical (■) and basolateral (▲) loading. Data are mean \pm s.d. (*n* = 3).

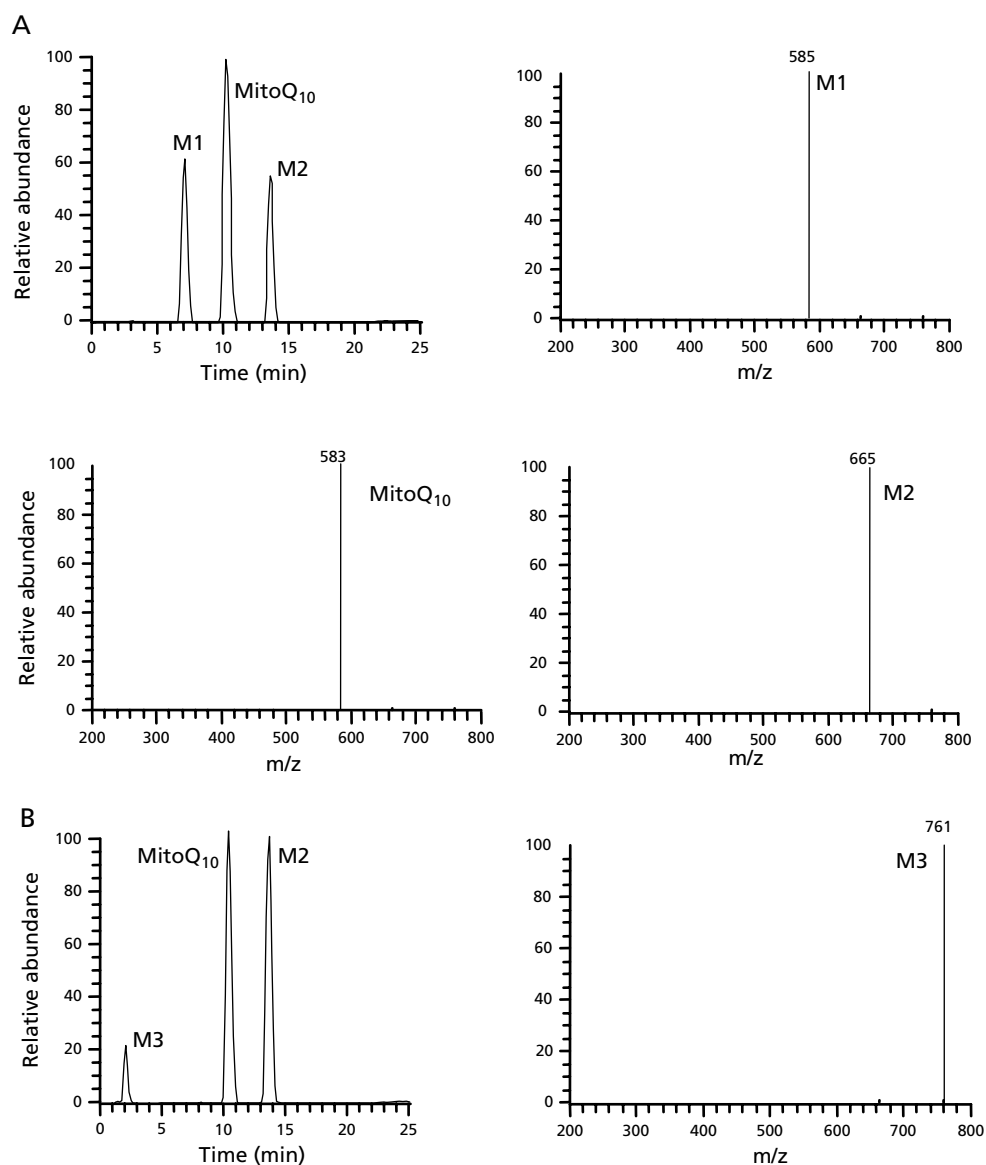


Figure 3 LC-MS chromatograms and spectra of the samples from cell homogenates (A) and apical buffer (B) at the end of a transport experiment with MitoQ₁₀.

disappeared and the MitoQ₁₀ peak increased. However, there was no significant change in the M2 peak after treatment with sulfatase.

The identity of these metabolites was further confirmed by LC-MS² experiments. The MS² product ion spectrum (Figure 4b) of M1 was identical to that of an authentic specimen of mitoquinol (Figure 4a). Fragment ions were present at *m/z* 570, 555 and 387, indicative of the loss of: one CH₃; one CH₂O; one CH₂, one CH₂O and two C₆H₅, respectively. The MS² product ion spectrum of M2 and M3 showed an ion at *m/z* 585 (Figure 5), corresponding to the loss of one sulfate and one glucuronic acid, respectively. Both phase II metabolites were found in the donor and receiver chambers of the Caco-2 transport system (Figure 5).

Transport of MitoQ₁₀ and its phase II metabolites

As shown in Table 1, transport of MitoQ₁₀ was polarized with efflux ratios of 4.1, 3.8 and 2.7 at concentrations of 10, 20 and 30 μ M, respectively. In the presence of P-glycoprotein (P-gp) inhibitors, the $P_{appBL \rightarrow AP}$ value of MitoQ₁₀ was decreased 26% by verapamil (100 μ M), and 31 and 61% by cyclosporin 10 and 30 μ M, respectively. The $P_{appAP \rightarrow BL}$ value of MitoQ₁₀ was increased 71% by cyclosporin (30 μ M). However, the effects of decynium 22 (4 μ M) (a potent inhibitor of the organic cation transporter (OCT) (Grundemann et al 1999)), indometacin (150 μ M) (an inhibitor of multiple resistance protein (MRP) (Petri et al 2004)) and reserpine (25 μ M)

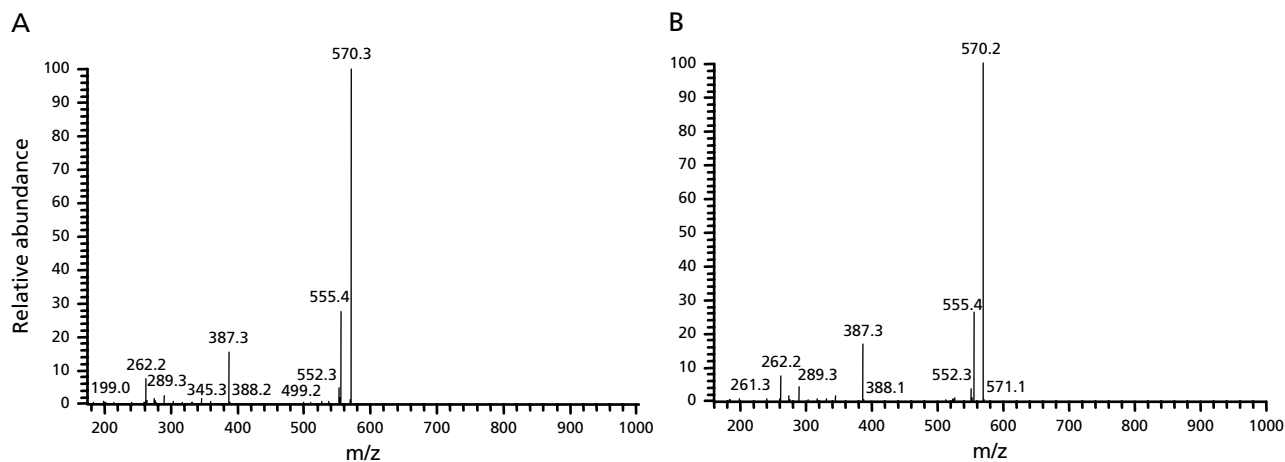


Figure 4 LC-MS/MS fragment ion spectra of synthesized mitoquinol (A) and M1 (B) in Figure 3.

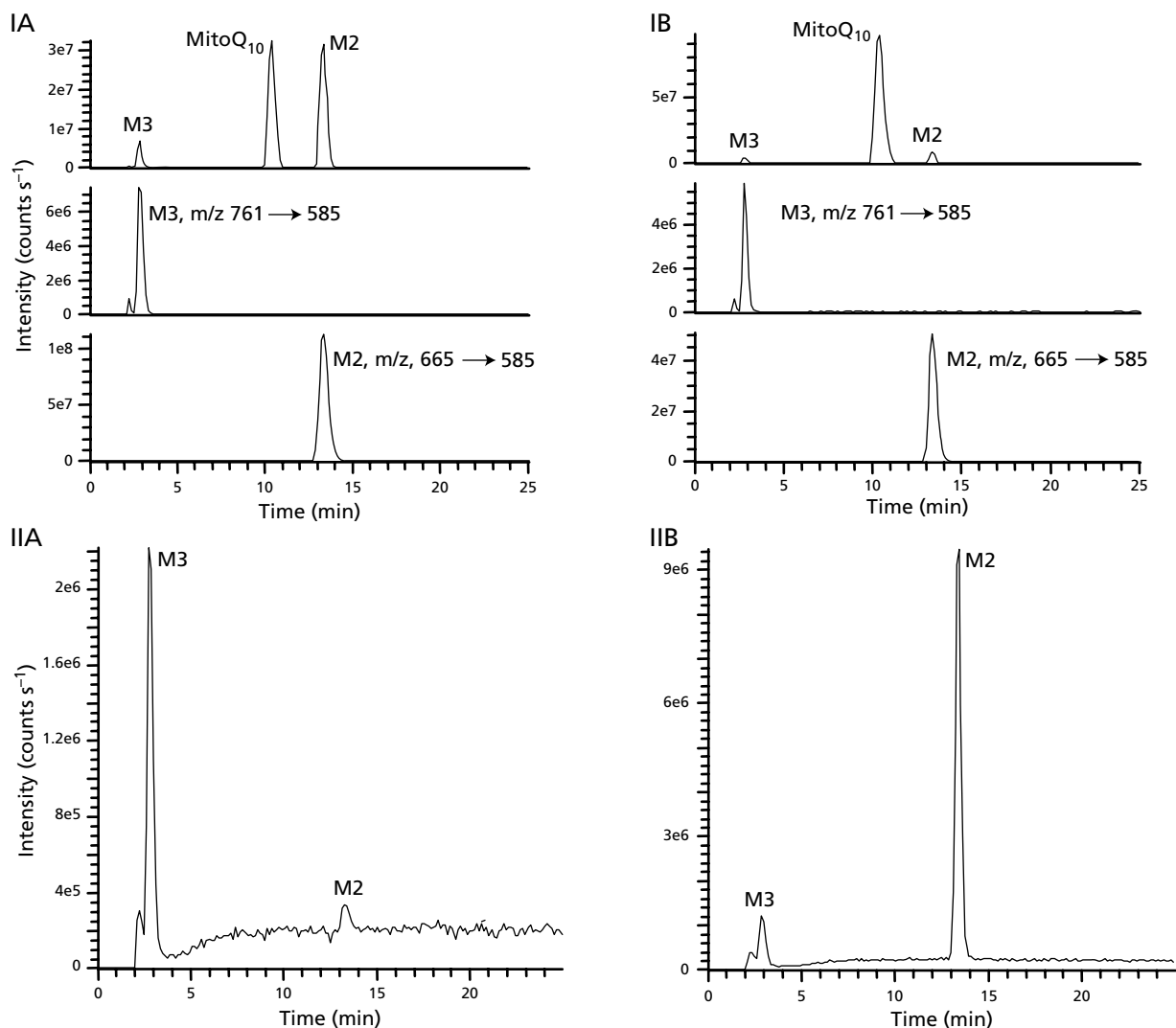


Figure 5 LC-MS chromatograms of samples taken from the donor (I) and receiver (II) sides at the end of a transport experiment. Ia, Apical loading and sampling; Ib, basolateral loading and sampling. Both upper traces of IA and IB show LC-MS chromatograms, and middle and lower traces show tandem MS product ion chromatograms of the metabolites (M2, monosulfated mitoquinol; M3, monoglucuronidated mitoquinol) found on the loading side. IIA, Apical loading and basolateral sampling; IIB, basolateral loading and apical sampling.

Table 1 P_{app} values (mean \pm s.d., $n=3$) of MitoQ₁₀ (10 μ M) in the absence and presence of various drug transporter inhibitors. The results for 20 and 30 μ M MitoQ₁₀ concentrations are also shown

	Apical to basolateral $P_{app} \pm$ s.d. ($\times 10^{-6}$ cm s ⁻¹)	Basolateral to apical $P_{app} \pm$ s.d. ($\times 10^{-6}$ cm s ⁻¹)	Efflux ratio
MitoQ ₁₀ (30 μ M)	0.71 \pm 0.07*	1.91 \pm 0.23*	2.67
MitoQ ₁₀ (20 μ M)	0.50 \pm 0.09	1.99 \pm 0.13*	3.76
MitoQ ₁₀ (10 μ M) (Control)	0.38 \pm 0.05	1.57 \pm 0.24	4.11
+ Cyclosporin (10 μ M)	0.47 \pm 0.05	1.08 \pm 0.14*	2.30
+ Cyclosporin (30 μ M)	0.65 \pm 0.08*	0.64 \pm 0.13**	0.99
+ Verapamil (100 μ M)	0.48 \pm 0.11	1.16 \pm 0.07*	2.42
+ Decynium 22 (4 μ M)	0.47 \pm 0.12	1.36 \pm 0.18	2.89
+ Indometacin (150 μ M)	0.44 \pm 0.09	1.62 \pm 0.23	3.68
+ Reserpine (25 μ M)	0.51 \pm 0.12	1.38 \pm 0.29	2.71

* $P < 0.05$; ** $P < 0.01$, compared with control.

(an inhibitor of breast cancer receptor protein (BCRP) (Ebert et al 2005)), on bidirectional transport were not significant (Table 1). In another set of experiments, the $P_{appAP \rightarrow BL}$ for MitoQ₁₀ (20 μ M) was increased 7-fold ($4.52 \pm 0.92 \times 10^{-6}$ cm s⁻¹ vs $0.62 \pm 0.12 \times 10^{-6}$ cm s⁻¹, $n=3$) in the presence of 4% BSA on the receiver side without concomitant change of [¹⁴C]mannitol permeability ($0.77 \pm 0.08 \times 10^{-6}$ vs $0.69 \pm 0.07 \times 10^{-6}$ cm s⁻¹, $n=3$).

Both sulfate and glucuronide metabolites were preferentially excreted to the apical side of Caco-2 cell monolayers after apical loading of MitoQ₁₀ (Figure 5). The excretion of monosulfated mitoquinol to the apical side was significantly decreased by cyclosporin (30 μ M), and apical efflux of monoglucuronidated mitoquinol significantly decreased by reserpine (25 μ M) (Figure 6).

Mass balance of [³H]MitoQ₁₀

The [³H]MitoQ₁₀ mass balance (without BSA on the receiver side) determined after transport studies was 82.9% \pm 5.9% ($n=3$) and 103.1% \pm 11.3% ($n=3$) at loading concentrations of 10 and 20 μ M, respectively.

Discussion

The extent of cellular uptake of MitoQ₁₀ is presumably described by the Nernst equation (Smith et al 2003). Kelso et al (2001) reported that the accumulation of MitoQ₁₀ at a loading concentration of 5 μ M by osteosarcoma 143-B cells was up to 450 pmol/ 5×10^6 cells in 2 h. Using a cell volume of 0.88 pL/cell (Porteous et al 1998), this corresponded to 10.2×10^{-5} pmol pL⁻¹, in close agreement with the uptake of MitoQ₁₀ (9.7×10^{-5} pmol pL⁻¹) by Caco-2 cells. The accumulation of MitoQ₁₀ after apical loading was approximately 2–5-fold lower than after basolateral loading. This difference was possibly due to apical active efflux mediated by drug transporters such as P-gp rather than to any effect of OCTs, since the potent OCT inhibitor, decynium 22 (4 μ M) had little effect on either apical or basolateral uptake (data not shown)

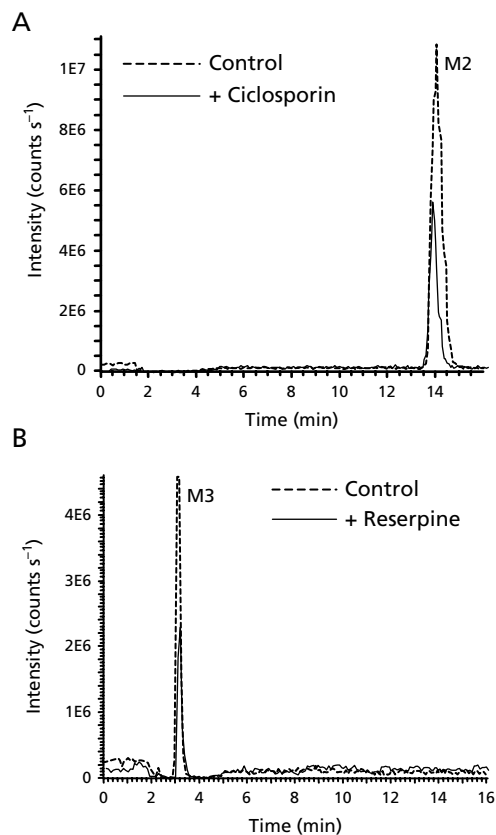


Figure 6 Extract ion chromatograms of samples taken from the apical side 1 h after apical loading of MitoQ₁₀. A, Monosulfated mitoquinol (M2) on the apical side with (solid line) and without (dashed line) cyclosporin (30 μ M); B, monoglucuronidated mitoquinol (M3) on the apical side with (solid line) and without (dashed line) reserpine (25 μ M).

or bidirectional transport (Table 1) of MitoQ₁₀. As P-gp is localized on the apical membrane of Caco-2 cells, uptake of substrate from the apical side may be more difficult than from the basolateral side.

P-gp (MDR1 in man) is a multidrug efflux transporter that pumps lipophilic, mostly cationic, solutes out of the cell (Litman et al 2001). P-gp is expressed on the apical side of the intestinal epithelium and its activity results in limited oral absorption of several cationic compounds (such as vinblastine, epirubicin and talinolol) in man (Sikic et al 1997; Schwarz et al 2000; Bogman et al 2005). Evidence for the involvement of P-gp in the efflux of MitoQ₁₀ includes: polarized transport, as indicated by a 2–4-fold greater basolateral-to-apical than apical-to-basolateral transport; a significant inhibition in basolateral to apical transport by cyclosporin and verapamil; and a significant increase in apical to basolateral transport by cyclosporin. It is reported that P-gp-mediated efflux activity may be inhibited more readily when the substrate approaches from the basolateral side rather than the apical side (Troutman & Thakker 2003). This may explain why verapamil (100 μ M) inhibited basolateral-to-apical efflux of MitoQ₁₀ but had little effect on apical-to-basolateral transport.

However, even with complete inhibition of P-gp activity by cyclosporin (efflux ratio decreased to 0.99, Table 1), the

$P_{appAP \rightarrow BL}$ value was still low and similar to model compounds with incomplete oral absorption (Artursson & Karlsson 1991). This suggested other factors may have limited the transport of MitoQ₁₀ across Caco-2 monolayers. MitoQ₁₀ is a lipophilic (log P 3.4) (Asin-Cayuela et al 2004) and a highly protein bound compound (plasma protein binding >95%, unpublished data). After transport studies, the apical uptake of MitoQ₁₀ was 18–26% of the total added amount at the loading concentrations of 2.5–30 μ M. The low $P_{appAP \rightarrow BL}$ value and significant cellular accumulation of MitoQ₁₀ suggests it undergoes slow partitioning from the Caco-2 basolateral membrane to the basolateral buffer. Our results were similar to those reporting that increased cellular accumulation led to decreased transcellular diffusion across Caco-2 cell monolayers (Wils et al 1994; Aungst et al 2000). In another permeability study using Madin-Darby canine kidney (MDCK) cell monolayers, when the cellular accumulation of lipophilic pyrrolopyrimidines was >2% of loading dose (7.5-fold the MitoQ₁₀ loading dose), decreased permeability was observed (Sawada et al 1999).

However, in the presence of 4% BSA in the basolateral buffer (mimicking the plasma albumin level in man), the MitoQ₁₀ $P_{appAP \rightarrow BL}$ value increased 7-fold without a concomitant change in [¹⁴C]mannitol permeability. Similarly, it was reported that basolateral BSA increased absorptive permeability of compounds with log P > 3 and plasma protein binding > 95% (Aungst et al 2000). Therefore, it has been suggested that the presence of BSA on the basolateral side provides a better in-vitro–in-vivo correlation when predicting in-vivo oral absorption of lipophilic, highly protein bound compounds (Sawada et al 1999; Aungst et al 2000; Saha & Kou 2002). MitoQ₁₀ is such a compound with a log P of 3.4 and plasma protein binding > 95%. With BSA in the basolateral side, the MitoQ₁₀ $P_{appAP \rightarrow BL}$ was $4.52 \pm 0.92 \times 10^{-6}$ cm s⁻¹. Drugs with $P_{appAP \rightarrow BL}$ in this range are reported to be highly absorbed in man (Artursson et al 2001; Saha & Kou 2002), suggesting that MitoQ₁₀ may be well absorbed orally. In the presence of BSA, intracellular MitoQ₁₀ decreased, and both intracellular and extracellular monosulfated mitoquinol dramatically dropped (data not shown). Published results suggested that the BSA increased absorptive permeability by reducing cellular accumulation (Sawada et al 1999; Aungst et al 2000). Decreased cellular accumulation may also lead to limited efficiency of intestinal metabolism of a drug. For example, intestinal metabolism of midazolam by CYP3A4-expressing Caco-2 cells was decreased in the presence of basolateral BSA (Fisher et al 1999). Thus the presence of BSA in the basolateral side could have provided a sink similar to in-vivo. An alternative role of BSA is that it could reduce adsorption of MitoQ₁₀ to the plastic well (Krishna et al 2001). However, our [³H]MitoQ₁₀ mass balance study showed limited non-specific drug binding to the plastic wells, thus the effects of BSA are most likely due to better sink conditions.

Mitoquinol was identified in Caco-2 cell homogenates suggesting that the quinone moiety was reduced during transcellular transport of MitoQ₁₀. Quinone reductase (NQO1) mostly resides in the cytosolic fraction of the cell where it can reduce ubiquinone to ubiquinol (Beyer et al 1996). However, the reduction of MitoQ₁₀ in Caco-2 cells could not have been

catalysed by NQO1 since it was inactive in Caco-2 cells (Karczewski et al 1999). It was recently demonstrated that MitoQ₁₀ was reduced to mitoquinol by Complex II and glycerol 3-phosphate dehydrogenase inside mitochondria (James et al 2005). Zhang et al (1996) reported functional expression of mitochondrial Complex II succinate dehydrogenase in Caco-2 cells. As MitoQ₁₀ can significantly accumulate into mitochondria (Kelso et al 2001), mitochondrial metabolism of MitoQ₁₀ to mitoquinol may occur inside Caco-2 cells.

The identity of monoglucuronidated mitoquinol was confirmed by enzymatic hydrolysis and LC-MS², whereas monosulfated mitoquinol, identified by LC-MS², was not cleaved by sulfatase. It has been shown that the presence of substituent groups ortho to the position of a sulfate ester group can hinder its hydrolysis by some sulfatases (Mulder 1984). This may explain the resistance to hydrolysis of monosulfated mitoquinol.

Accumulating evidence has demonstrated that Caco-2 cells retain functionally-active phase II metabolic enzymes, including uridine diphosphoglucuronosyl transferase (UGT), sulfotransferase (SULT) and glutathione-S-transferase (GST) (Chikhale & Borchardt 1994; Prueksaritanont et al 1996; Zhang et al 2004). The metabolites found in this study suggested that MitoQ₁₀ may undergo similar metabolism during absorption in the human small intestine. However, both the amounts (Sun et al 2002) and activity (Prueksaritanont et al 1996) of these phase II metabolizing enzymes in Caco-2 cells appeared to be lower than in-vivo. On the other hand, binding of MitoQ₁₀ to plasma protein in-vivo may accelerate absorptive transport, leading to decreased cellular accumulation and thus limited intestinal metabolism. Thus the data generated in the Caco-2 cell model may not quantitatively predict the extent of intestinal metabolism of orally administered MitoQ₁₀ in man.

Efflux of phase II metabolites of MitoQ₁₀ was preferentially to the apical side. According to our inhibition studies, monoglucuronidated mitoquinol was a BCRP substrate whereas monosulfated mitoquinol was a P-gp substrate. BCRP, like P-gp, is an efflux pump expressed on the apical side of the human small intestine and Caco-2 cells (Xia et al 2005). It can transport drugs as well as several phase II metabolites such as estrone sulfate, benzo[a]pyrene-3-glucuronide and 4-methylumbelliferone glucuronide (Suzuki et al 2003; Ebert et al 2005). Thus P-gp and BCRP may function as barriers to absorption of MitoQ₁₀ in-vivo by cooperating with phase II metabolic enzymes.

Conclusion

During transport, MitoQ₁₀ accumulated in human intestinal Caco-2 cells where it underwent metabolism to mitoquinol, monoglucuronidated mitoquinol and monosulfated mitoquinol. In-vitro transport studies in Caco-2 cell monolayers suggested MitoQ₁₀ and monosulfated mitoquinol would be subject to intestinal efflux by P-gp, whereas monoglucuronidated mitoquinol would undergo a similar fate due to BCRP. However, the dramatic increase in absorptive P_{app} in the presence of BSA on the receiver side suggests these barrier functions may have been less significant for orally administered MitoQ₁₀ in-vivo than predicted in-vitro.

References

- Adlam, V. J., Harrison, J. C., Porteous, C. M., James, A. M., Smith, R. A. J., Murphy, M. P., Sammut, I. A. (2005) Targeting an antioxidant to mitochondria decreases cardiac ischemia-reperfusion injury. *FASEB J.* **19**: 1088–1095
- Artursson, P., Karlsson, J. (1991) Correlation between oral drug absorption in humans and apparent drug permeability coefficients in human intestinal epithelial (Caco-2) cells. *Biochem. Biophys. Res. Commun.* **175**: 880–885
- Artursson, P., Palm, K., Luthman, K. (2001) Caco-2 monolayers in experimental and theoretical predictions of drug transport. *Adv. Drug Deliv. Rev.* **46**: 27–43
- Asin-Cayuela, J., Manas, A. R., James, A. M., Smith, R. A., Murphy, M. P. (2004) Fine-tuning the hydrophobicity of a mitochondria-targeted antioxidant. *FEBS Lett.* **571**: 9–16
- Aungst, B. J., Nguyen, N. N., Bulgarelli, J. P., Oates-Lenz, K. (2000) The influence of donor and reservoir additives on Caco-2 permeability and secretory transport of HIV protease inhibitors and other lipophilic compounds. *Pharm. Res.* **17**: 1175–1180
- Beyer, R. E., Segura-Aguilar, J., Di Bernardo, S., Cavazzoni, M., Fato, R., Fiorentini, D., Galli, M. C., Setti, M., Landi, L., Lenaz, G. (1996) The role of DT-diaphorase in the maintenance of the reduced antioxidant form of coenzyme Q in membrane systems. *Proc. Natl. Acad. Sci. USA* **93**: 2528–2532
- Bleyer, W. A., Danielson, M. (1999) Oral cancer chemotherapy in paediatric patients: obstacles and potential for development and utilisation. *Drugs* **58** (Suppl. 3): 133–140
- Bogman, K., Zysset, Y., Degen, L., Hopfgartner, G., Gutmann, H., Alsenz, J., Drewe, J. (2005) P-glycoprotein and surfactants: effect on intestinal talinolol absorption. *Clin. Pharmacol. Ther.* **77**: 24–32
- Chikhale, P. J., Borchardt, R. T. (1994) Metabolism of L-alpha-methyl dopa in cultured human intestinal epithelial (Caco-2) cell monolayers – comparison with metabolism in vivo. *Drug Metab. Dispos.* **22**: 592–600
- DeMario, M., Ratain, M. (1998) Oral chemotherapy: rationale and future directions. *J. Clin. Oncol.* **17**: 3362–3365
- Doppenschmitt, S., Spahn-Langguth, H., Regardh, C. G., Langguth, P. (1999) Role of P-glycoprotein-mediated secretion in absorptive drug permeability: an approach using passive membrane permeability and affinity to P-glycoprotein. *J. Pharm. Sci.* **88**: 1067–1072
- Ebert, B., Seidel, A., Lampen, A. (2005) Identification of BCRP as transporter of benzo[a]pyrene conjugates metabolically formed in Caco-2 cells and its induction by Ah-receptor agonists. *Carcinogenesis* **26**: 1754–1763
- Fisher, J. M., Wrighton, S. A., Calamia, J. C., Shen, D. D., Kunze, K. L., Thummel, K. E. (1999) Midazolam metabolism by modified Caco-2 monolayers: effects of extracellular protein binding. *J. Pharmacol. Exp. Ther.* **289**: 1143–1150
- Gan, L. S. L., Thakker, D. R. (1997) Applications of the Caco-2 model in the design and development of orally active drugs – elucidation of biochemical and physical barriers posed by the intestinal epithelium. *Adv. Drug Deliv. Rev.* **23**: 77–98
- Grundemann, D., Liebich, G., Kiefer, N., Koster, S., Schomig, E. (1999) Selective substrates for non-neuronal monoamine transporters. *Mol. Pharmacol.* **56**: 1–10
- James, A. M., Cocheme, H. M., Smith, R. A., Murphy, M. P. (2005) Interactions of mitochondria-targeted and untargeted ubiquinones with the mitochondrial respiratory chain and reactive oxygen species. Implications for the use of exogenous ubiquinones as therapies and experimental tools. *J. Biol. Chem.* **280**: 21295–21312
- Jauslin, M. L., Meier, T., Smith, R. A. J., Murphy, M. P. (2003) Mitochondria-targeted antioxidants protect Friedreich ataxia fibroblasts from endogenous oxidative stress more effectively than untargeted antioxidants. *FASEB J.* **17**: 1972–1974
- Karczewski, J. M., Peters, J. G. P., Noordhoek, J. (1999) Quinone toxicity in DT-diaphorase-efficient and -deficient colon carcinoma cell lines. *Biochem. Pharmacol.* **57**: 27–37
- Kelso, G. F., Porteous, C. M., Coulter, C. V., Hughes, G., Porteous, W. K., Ledgerwood, E. C., Smith, R. A. J., Murphy, M. P. (2001) Selective targeting of a redox-active ubiquinone to mitochondria within cells. Antioxidant and anti-apoptotic properties. *J. Biol. Chem.* **276**: 4588–4596
- Krishna, G., Chen, K. W. J., Lin, C. C., Nomeir, A. A. (2001) Permeability of lipophilic compounds in drug discovery using in-vitro human absorption model, Caco-2. *Int. J. Pharm.* **222**: 77–89
- Litman, T., Druley, T. E., Stein, W. D., Bates, S. E. (2001) From MDR to MXR: new understanding of multidrug resistance systems, their properties and clinical significance. *Cell Mol. Life Sci.* **58**: 931–959
- Matsson, P., Bergstrom, C. A., Nagahara, N., Tavelin, S., Norinder, U., Artursson, P. (2005) Exploring the role of different drug transport routes in permeability screening. *J. Med. Chem.* **48**: 604–613
- Mulder, G. J. (1984) Sulfation—metabolic aspects. In: Bridges, J. W., Chasseaud, L. F. (eds) *Progress in drug metabolism*. Taylor & Francis Ltd, New York; 8, pp 35–100
- Murphy, M. P., Smith, R. A. J. (2000) Drug delivery to mitochondria: the key to mitochondrial medicine. *Adv. Drug Deliv. Rev.* **41**: 235–250
- Nyholm, D. (2006) Pharmacokinetic optimisation in the treatment of Parkinson's disease: an update. *Clin. Pharmacokinet.* **45**: 109–136
- Petri, N., Tannergren, C., Rungstad, D., Lennernas, H. (2004) Transport characteristics of fexofenadine in the Caco-2 cell model. *Pharm. Res.* **21**: 1398–1404
- Porteous, W. K., James, A. M., Sheard, P. W., Porteous, C. M., Packer, M. A., Hyslop, S. J., Melton, J. V., Pang, C.-Y., Wei, Y.-H., Murphy, M. P. (1998) Bioenergetic consequences of accumulating the common 4,977 bp mitochondrial DNA deletion. *Eur. J. Biochem.* **257**: 192–201
- Pruksaritanont, T., Gorham, L. M., Hochman, J. H., Tran, L. O., Vyas, K. P. (1996) Comparative studies of drug-metabolizing enzymes in dog, monkey, and human small intestines, and in Caco-2 cells. *Drug Metab. Dispos.* **24**: 634–642
- Saha, P., Kou, J. H. (2002) Effect of bovine serum albumin on drug permeability estimation across Caco-2 monolayers. *Eur. J. Pharm. Biopharm.* **54**: 319–324
- Sawada, G. A., Barsuhn, C. L., Lutzke, B. S., Houghton, M. E., Padbury, G. E., Ho, N. F. H., Raub, T. J. (1999) Increased lipophilicity and subsequent cell partitioning decrease passive transcellular diffusion of novel, highly lipophilic antioxidants. *J. Pharmacol. Exp. Ther.* **288**: 1317–1326
- Schwarz, U., Gramatte, T., Krappweis, J., Oertel, R., Kirch, W. (2000) P-glycoprotein inhibitor erythromycin increases oral bioavailability of talinolol in humans. *Int. J. Clin. Pharmacol. Ther.* **38**: 161–167
- Sikic, B., Fisher, G., Lum, B., Halsey, J., Beketic-Oreskovic, L., Chen, G. (1997) Modulation and prevention of multidrug resistance by inhibitors of P-glycoprotein. *Cancer Chemother. Pharmacol.* **40** (Suppl.): 13–19
- Smith, R. A. J., Porteous, C. M., Gane, A. M., Murphy, M. P. (2003) Delivery of bioactive molecules to mitochondria in vivo. *Proc. Natl. Acad. Sci. USA* **100**: 5407–5412
- Stoof, J. C., Winogrodzka, A., van Muiswinkel, F. L., Wolters, E. C., Voorn, P., Groenewegen, H. J., Booij, J., Drukarch, B. (1999) Leads for the development of neuroprotective treatment in Parkinson's disease and brain imaging methods for estimating treatment efficacy. *Eur. J. Pharmacol.* **375**: 75–86
- Sun, D., Lennernas, H., Welage, L., Barnett, J., Landowski, C., Foster, D., Fleisher, D., Lee, K., Amidon, G. (2002) Comparison

- of human duodenum and Caco-2 gene expression profiles for 12,000 gene sequences tags and correlation with permeability of 26 drugs. *Pharm. Res.* **19**: 1400–1416
- Suzuki, M., Suzuki, H., Sugimoto, Y., Sugiyama, Y. (2003) ABCG2 transports sulfated conjugates of steroids and xenobiotics. *J. Biol. Chem.* **278**: 22644–22649
- Troutman, M. D., Thakker, D. R. (2003) Novel experimental parameters to quantify the modulation of absorptive and secretory transport of compounds by P-glycoprotein in cell culture models of intestinal epithelium. *Pharm. Res.* **20**: 1210–1224
- Wils, P., Warnery, A., Phung-Ba, V., Legrain, S., Scherman, D. (1994) High lipophilicity decreases drug transport across intestinal epithelial cells. *J. Pharmacol. Exp. Ther.* **269**: 654–658
- Xia, C. Q., Liu, N., Yang, D., Miwa, G., Gan, L. S. (2005) Expression, localization, and functional characteristics of breast cancer resistance protein in Caco-2 cells. *Drug Metab. Dispos.* **33**: 637–643
- Yee, S. (1997) In vitro permeability across Caco-2 cells (colonic) can predict in vivo (small intestinal) absorption in man – fact or myth. *Pharm. Res.* **14**: 763–766
- Zhang, T. M., Jijakli, H., Malaisse, W. J. (1996) Nutritional efficiency of succinic acid and glutamic acid dimethyl esters in colon carcinoma cells. *Am. J. Physiol.* **270**: G852–859
- Zhang, L., Zheng, Y., Chow, M. S. S., Zuo, Z. (2004) Investigation of intestinal absorption and disposition of green tea catechins by Caco-2 monolayer model. *Int. J. Pharm.* **287**: 1–12

